Atmos. Meas. Tech. Discuss., 5, 325–350, 2012
www.atmos-meas-tech-discuss.net/5/325/2012/
doi:10.5194/amtd-5-325-2012

Atmospheric Measurement Techniques Discussions

New Aura Microwave Limb Sounder observations of BrO and implications for Br_y

L. Millán[1], N. Livesey[1], W. Read[1], L. Froidevaux[1], D. Kinnison[2], R. Harwood[3], I. A. MacKenzie[3], and M. P. Chipperfield[4]

[1]Jet Propulsion Laboratory, California Institute of Technology, Pasadena, California, USA
[2]National Center for Atmospheric Research, Boulder, Colorado, USA
[3]School of GeoSciences, University of Edinburgh, UK
[4]Institute for Climate and Atmospheric Science, University of Leeds, UK

Received: 10 December 2011 – Accepted: 20 December 2011 – Published: 10 January 2012

Correspondence to: L. Millán (luis.f.millan@jpl.nasa.gov)

Published by Copernicus Publications on behalf of the European Geosciences Union.

Abstract

This paper introduces a new inversion algorithm for retrievals of stratospheric BrO from the Aura Microwave Limb Sounder. This version is based on the algorithm described by Livesey et al. (2006a) but designed to reduce a large bias presented in the previous MLS BrO datasets in the lower stratosphere and, therefore, to increase its useable pressure range. In this new version, vertical profiles of BrO were obtained in the 100 to 4.6 hPa pressure range extending the lower altitude limit of the MLS retrievals. A description of the retrieval methodology and an error analysis are presented. Single daily profile precision, when taking the ascending-descending (day-night) difference, was found to be up to 40 pptv while systematic error biases were estimated to be less than about 3 pptv. Monthly mean comparisons show broad agreement with other measurements as well as with state-of-the-art numerical models. We infer total inorganic Br_y using the measured MLS BrO to be 20.3 ± 4.5 pptv, which implies a contribution from Very Short Lived Substances to the stratospheric bromine budget of $\sim 5 \pm 4.5$ pptv.

1 Introduction

Stratospheric ozone destruction has been a great concern since 1985, when massive ozone loss over the Antarctic spring, the now famous "ozone hole", was reported (Farman et al., 1985). Extensive research, both theoretical and observational, showed that this ozone depletion was caused by complex chemical processes involving radicals containing chlorine and bromine. Unlike for chlorine, the stratospheric bromine budget is still not well understood. The fact that bromine depletes stratospheric ozone 45 to 66 times more efficiently than chlorine on a per atom basis (Sinnhuber et al., 2009) makes this budget an issue of great importance.

Stratospheric inorganic bromine (Br_y) sources can be classified as (e.g., Wamsley et al., 1998; Montzka et al., 2003): natural and anthropogenic methyl bromide (CH_3Br), man made long-lived halons (such as $CBrClF_2$ and CBr_2F_2) and a variety of natural

AMTD
5, 325–350, 2012

Very Short Lived Substances (VSLS) containing bromine (such as $CHBr_3$, CH_2Br_2, CH_2ClBr). These compounds, when transported to the upper troposphere and stratosphere, are converted into inorganic bromine forms ($Br_y = Br + BrO + BrONO_2 + HOBr + BrCl + HBr$) by photolysis or reactions with OH radicals (e.g., Pundt et al., 2002).

Part of the reason why the stratospheric bromine budget is not well understood is that, despite many studies, the exact contribution of VSLS to the stratospheric Br_y is still uncertain; current estimates for the Br_y loading from VSLS vary from 3 to 8 pptv WMO (World Meteorological Organization, 2010, Chapt. 1). Furthermore, Salawitch et al. (2005) and Feng et al. (2007) have shown that even only a few pptv of additional bromine increases ozone depletion, especially during times of elevated stratospheric aerosol loading due to volcanic activities.

In this paper we introduce a new dataset of global observations of stratospheric BrO from the Aura Microwave Limb Sounder (MLS) instrument. BrO is the most abundant Br_y species during daytime and it has been used to estimate the stratospheric Br_y directly using photochemical models. We compare this new dataset with previous MLS BrO products, with expectations, and with other datasets. In addition, we infer a new estimate for the Br_y^{VSLS} loading.

2 MLS BrO observations

Aura was launched into a polar sun synchronous orbit on July 2004. As part of its payload, the MLS instrument measures thermal limb emission in the millimeter and submillimeter wavelength range. MLS scans the Earth's limb from the ground to about 95 km roughly 3500 times per day. It observes between 82° S and 82° N providing near-global coverage. In general, most measurements are made at about 01:45 or 13:45 local solar time (LST); the exceptions are the measurements near the poles where the satellite changes between day time and night time conditions or vice versa. A detailed description of the Aura MLS instrument is given by Waters et al. (1999) and Waters et al. (2006).

AMTD
5, 325–350, 2012

MLS collects the atmospheric radiation with a 1.6 m antenna and directs it onto four heterodyne radiometers covering spectral regions near 118, 191, 240 and 640 GHz (A fifth radiometer located at 2.5 THz is fed by a separate antenna). The outputs of the GHz radiometers are analyzed by 22 filter banks and 4 digital autocorrelator spectrometers (DACS). Each filter bank targets one molecule in particular, although MLS is a double sideband receiver that simultaneously observes two separate spectral regions; when possible, the overlapping regions were chosen with no strong lines.

MLS observes two sets of BrO emission lines in the 640 GHz radiometer with two filter banks, one around 650 GHz and the other around 625 GHz. Figure 1 shows observations from these filter banks. In the two cases the ~0.2 K BrO signal overlaps with a ~2 K O_3 signal. Taking the ascending-descending (day-night) difference removes the O_3 signal, which does not have a diurnal variation at these altitudes, revealing the strongly diurnal nature of BrO. Furthermore the ~0.2 K BrO signal is well below the individual measurement precision of about 4 K, hence, significant averaging is required to obtain a useful BrO signal.

3 Retrieval methodology

To date, two different approaches to do the required averaging have been implemented. The standard production approach (MLS L2) is simply to retrieve the BrO abundances for every limb sequence and then average the individual profiles (see Kovalenko et al., 2007). This approach produces approximately 3500 profiles daily with a 10° monthly zonal mean precision of ~4 pptv. These retrieval algorithms are described in detail by Livesey et al. (2006b). In summary, the well known optimal estimation technique (Rodgers, 2000) is used employing a two-dimensional approach that uses consecutive scans covering overlapping regions of the atmosphere along the sub-orbital track. In the current version (version 3.3), the BrO abundances are retrieved simultaneously with several other molecules (ClO, HCl, O_3, HO_2, HOCl, CH_3CN, HNO_3, SO_2 and

AMTD
5, 325–350, 2012

CH_3Cl) using all the available radiances in the 640 GHz radiometer. The temperature, pressure, and pointing information are retrieved in a previous stage.

The second approach, performed "off-line" (MLS OL1), is to create daily zonal mean radiances from which vertical BrO abundances can then be retrieved. This approach was implemented by Livesey et al. (2006a). In short, limb scans from a particular day are collocated into 10° latitude average bins sorting them into ascending (mostly daytime) and descending (mostly nighttime) parts of the orbit. Radiances are binned onto a vertical grid of 6 surfaces per decade change in pressure (~1.5 km) using the limb tangent pressure from the standard production data. This retrieval uses a one-dimensional optimal estimation technique producing a pair of zonal mean abundances for each day (one ascending and one descending) giving a 10° monthly zonal mean precision of ~3.5 pptv. This algorithm retrieves temperature and some BrO overlapping species simultaneously from only the 650 and 625 GHz filter banks.

For this study, a new "off-line" algorithm has been developed (MLS OL2). It is similar to the one described by Livesey et al. (2006a) with the following differences: (1) this retrieval uses averaged temperature, O_3, and HNO_3 data from the standard production algorithm, (2) minor overlapping species are retrieved independently for each band, and (3) the channels used in each BrO spectral band were more carefully selected. This selection was performed by searching for consistency in the BrO abundances retrieved from each band.

For comparison, Fig. 2 shows monthly zonal means for the three versions previously discussed. MLS L2 exhibits a large negative offset for pressures larger than 10 hPa. The two "off-line" algorithms display similar behaviors, however MLS OL1 still shows a hint of this negative bias. These negative offsets have so far restricted the maximum usable pressure level to 10 hPa. As shown, the MLS OL2 retrievals do not display this problem, extending the usable vertical range downward to 100 hPa.

As previously discussed by Livesey et al. (2006a) and Kovalenko et al. (2007), negligible BrO abundances are expected at mid and equatorial latitudes for pressures larger than ~4 hPa during night, hence non-zero descending BrO retrieved abundances at

AMTD
5, 325–350, 2012

these pressure levels indicate biases caused by improperly modelled systematic errors. These systematic errors are expected to be constant irrespective of the solar illumination, hence, an ascending-descending BrO difference significantly reduces these systematic errors. This difference is therefore a better estimate of the daytime BrO than taking just the face values of the ascending set. Unfortunately, this restricts the usable data of any of the MLS BrO products to between 50° S and 50° N, with a minimum usable pressure of 4.6 hPa. As pointed out by Kovalenko et al. (2007), it may be possible to characterize these systematic errors in order to reduce the biases in the polar regions and extend the coverage of the MLS data. As displayed in Fig. 2, there is no indication of significant systematic biases in the ascending-descending subplot for the new retrievals presented here.

3.1 Vertical resolution

Typical averaging kernels for the retrieval of BrO are shown in Fig. 3. They describe how the true state of the atmosphere has been distorted by the retrieval at each pressure level. The half width of each kernel provides a measure of the vertical resolution of the retrieval, and its area (the integrated kernel) indicates the dependence on the a priori.

3.2 Error assessment

The total error in the retrieved product arises from the sum of the random and systematic errors. The random errors (the expected precision) are determined by the random noise in the measurements while the systematic errors arise from forward model uncertainties, instrumental issues, and retrieval approximations.

Figure 4 displays the expected precision for daily, monthly, and yearly profiles over a 10° latitude bin. The ascending and descending precisions are very similar. Over a pressure range between 20 and 4 hPa, the daily precision for a 10° latitude bin either ascending or descending is around 25 pptv dropping to 5 pptv and below 2 pptv for

AMTD
5, 325–350, 2012

monthly and yearly averages, respectively. The precision in the ascending-descending difference is up to 40 pptv daily while the monthly and yearly precision drops to ∼7 and ∼2 pptv.

Two methods have been used to quantify the impact of the systematic errors. In the first method, the errors are estimated by an end-to-end simulation of the retrieval algorithm. First, for each systematic error, a perturbed set of radiance simulations is generated for a whole day (∼3500 profiles) using a model atmosphere (a complete list and more detailed discussion of the systematic errors is given by Read et al. (2007, Appendix A)). These simulated radiances were binned in 10° latitude bins and gridded onto a 6 surface per decade pressure grid and then run through the "off-line" retrieval algorithm as normal. Each of the retrieved results is compared to the retrieved BrO from an unperturbed run, as a measure of the impact of a given systematic error source. Each perturbation corresponds to either 2σ estimates of uncertainties in the relevant parameter or an estimate of their maximum reasonable error based on instrument knowledge. Furthermore, the difference between the unperturbed run and the model atmosphere estimates the errors due to approximations in the retrieval.

A second method is used for the typically small error sources that are difficult to quantify in an end-to-end exercise. Their impact is quantified with a simple analytical model of the MLS measurement system (Read et al., 2007, Auxiliary material).

Figure 5 summarizes the impact of the dominant systematic uncertainties for the BrO MLS OL2 measurements introduced here. Throughout most of the profile (either for the ascending or the descending case), the main source of systematic bias arises from retrieval numerics. While unsatisfactory this is somewhat expected due to strong overlapping O_3 signals in contrast to the small BrO signature, in addition to the smoothing inherent in the retrieval algorithm.

As already mentioned, the effects of the systematic biases can be diminished by subtracting the nighttime retrieved values from the daytime (taking advantage of the pronounce BrO diurnal variation below ∼4 hPa where negligible BrO is expected during night). Figure 6 summarizes the impact of several systematic uncertainties for the

AMTD
5, 325–350, 2012

MLS OL2 BrO measurements when the ascending-descending differences are used as an indicator of daytime BrO. Note that since averages over several days are needed to obtain a useful BrO signal, the additional noise-induced scatter introduced by the ascending-descending differences will average down.

4 Comparisons with numerical models

To gain an idea of the performance of the "off-line" algorithm introduced here, Figs. 7 and 8 show monthly mean comparisons between the MLS OL2 data and two state-of-the-art numerical models: SLIMCAT and WACCM. Two months were compared, January and July 2005, in order to compare BrO at two points in the seasonal cycle.

SLIMCAT (Chipperfield, 1999, 2006) is an off-line chemical transport model (CTM). For this analysis it was run driven by the European Centre for Medium-Range Weather Forecasts (ECMWF) winds and temperature fields with a horizontal resolution of $2.8^\circ \times 2.8^\circ$ and a vertical coordinate which, in the stratosphere, is essentially based on isentropic surfaces with a spacing of approximately 1.2 km. The model results were sampled at the same location and time as the MLS individual profiles. Reaction rates were taken from the JPL 2002 recommendations (Sander et al., 2003) with the added reaction (Soller et al., 2001).

$$BrONO_2 + O \rightarrow BrO + NO_3 \quad (1)$$

The Whole Atmosphere Community Climate Model (WACCM), Version 4 is a fully interactive chemistry climate model, where the radiatively active gases affect heating and cooling rates and therefore dynamics (Garcia et al., 2007). For this analysis the model was run with a horizontal resolution of $1.9^\circ \times 2.5^\circ$ in latitude and longitude using meteorological fields derived from the Goddard Earth Observing System 5 (GEOS-5) analyzes, and a vertical coordinate purely isobaric in the stratosphere with a variable spacing of 1.1 to 1.75 km. This new capability of this model is described by Lamarque et al. (2011) and allows WACCM to perform as a chemical transport module facilitating

AMTD
5, 325–350, 2012

the comparisons with observations. The chemical module of WACCM is based on the 3-D chemical transport Model of Ozone and Related Tracers, Version 4 (Kinnison et al., 2007). Reactions rates were taken from the JPL 2006 recommendations (Sander et al., 2006) which includes reaction 1.

As shown in Figs. 7 and 8, MLS OL2 data display the distinct BrO ~10 hPa diurnal variation not only at mid and equatorial latitudes but also at the poles with negligible BrO abundances around the polar winter regions (where there is constant nighttime) and higher BrO values in the polar summer regions (where there is constant daytime).

Furthermore, the MLS OL2 data also display the diurnal BrO variation at about 0.5 hPa, with high values at nighttime and negligible values during daytime. This suggests that a descending-ascending difference might be a good estimate of the nighttime BrO abundances for pressures smaller than 0.7 hPa where the expected daytime BrO is zero. However, due to the poor BrO signal to noise ratio, around these pressure levels the impact of the random errors are higher, hence, these data are not recommended for scientific use without previous consultation with the MLS science team.

5 Comparisons with other datasets

Comparison of monthly zonal means were made with those of the Scanning Imaging Absorption spectrometer for Atmospheric Cartography (SCIAMACHY) and the Optical Spectrograph and Infrared Imaging System (OSIRIS) instruments.

SCIAMACHY, on board the ENVISAT satellite launched in March 2002, is a spectrometer measuring solar radiation in the ultraviolet, the visible and the near infrared spectral regions (240–2380 nm) at a moderate spectral resolution (0.2–1.5 nm) either in nadir, solar/lunar occultation or limb viewing modes. These viewing modes are used during each orbit to retrieve tropospheric, stratospheric and mesospheric compositions. In this study we used the stratospheric BrO retrievals described by Rozanov et al. (2005), in particular version 3.2. These measurements have a local time of 10:00 a.m.

AMTD
5, 325–350, 2012

OSIRIS is on board the ODIN satellite launched in February 2001. From launch to April 2007, the Odin satellite was a multipurpose mission which alternated between astronomical and atmospheric measurements in one day bins (Lewellyn et al., 2004). Since April 2007, Odin is a full-time atmospheric satellite. OSIRIS measures spectra across the visible range from 274 nm to 810 nm every 0.3 nm using diffraction gratings. It scans the atmosphere from around 7 to 65 or 90 km, depending on the observing mode with an irregular vertical resolution. These measurements have local times of either 6 a.m. or 6 p.m. More information in the OSIRIS BrO retrieval can be found in McLinden et al. (2010).

Due to the diurnal nature of the BrO abundances, comparisons between measurements with different local times must be made with caution. Figure 9 shows BrO monthly means from MLS OL2, OSIRIS AM and SCIAMACHY for March and September 2005. These months were chosen to maximize the OSIRIS coverage. The values shown are the reported retrieved values and as such, this analysis should only be considered as a zero order comparison. As can be seen, the MLS data shows a similar vertical structure and magnitude to both datasets, with increasing BrO values as the pressure decreases. A more careful validation exercise would be to map one measurement to the others using box models constrained by local temperature and local O_3 and NO_2 abundances.

6 Implications for total Br_y

From MLS OL2 BrO measurements, Br_y can be inferred approximately from chemical models using the expression

$$Br_y^{MLS} = BrO^{MLS}\left(\frac{Br_y^{MODEL}}{BrO^{MODEL}}\right) \quad (2)$$

AMTD
5, 325–350, 2012

Figure 10 shows average Br_y profiles obtained using the WACCM and the SLIMCAT models. In addition, it also shows the WACCM and SLIMCAT Br_y for comparison. These profiles are a yearly average over 50° S and 50° N. Part of the difference between these profiles is that WACCM Br_y loading only includes the sum of CH_3Br and long-lived halons while SLIMCAT includes those two sources plus VSLS. As can be seen, the two Br_y^{MLS} estimates are in excellent agreement. These two yearly profiles of Br_y^{MLS} correspond to estimates of stratospheric Br_y of 20 ± 4.5 pptv and 20.6 ± 4.5 pptv (calculated over the pressure surfaces from 10 to 4.6 hPa) for the data derived with the WACCM and the SLIMCAT model, respectively. Since the two estimates are similar we assume the Br_y^{MLS} final estimate to be 20.3 ± 4.5 pptv.

Using a yearly mean of the MLS L2 N_2O measurements between 10 and 4.6 hPa for 2005, and the correlation between N_2O and mean age described by Engel et al. (2002), we estimated the age of this air to be 5 ± 1 yr. According to Montzka et al. (2003), tropospheric CH_3Br and long-lived halons, the other two Br_y sources besides VSLS, contributed 15.6 pptv to the total bromine at that time. This implies that the new MLS OL2 retrievals suggest a $\sim 5 \pm 4.5$ VSLS contribution to Br_y. Note that the error associated with this estimate is only a guidance since the errors induced by the models and the errors induced by the Montzka et al. (2003) estimate of the tropospheric CH_3Br and long-lived halons were neglected.

This VSLS contribution to Br_y is within the expected range (3 to 8 pptv) found in the 12 estimates of Br_y^{VSLS} discussed by WMO (2010) (chapter 1) and falls between the two previous MLS estimates 3 ± 5.5 (Livesey et al., 2006a) and 6.5 ± 5.5 pptv (Kovalenko et al., 2007).

7 Summary and conclusions

MLS zonal mean spectra divided into ascending (daytime) and descending (nighttime) were computed for each day and inverted to produce daily zonal mean BrO profiles from 100 to 4.6 hPa. Due to the sharp BrO diurnal variation, the MLS non-zero

AMTD
5, 325–350, 2012

descending BrO abundances were used as a measure of systematic biases in the retrievals. Assuming that these biases are constant throughout day and night, we used the difference between ascending and descending BrO as a more accurate measure of daytime BrO. This restricts the usable data to 50° S to 50° N, avoiding the polar regions where both ascending and descending orbits are either day (summer) or night (winter).

The vertical resolution of this dataset in the 100 to 4.6 hPa region was found to be approximately 5 km (derived from the full width at half maximum, FWHM, of the averaging kernels scaled into km). For this pressure range, single daily ascending-descending profile precision for a 10° latitude bin was found to be up to 40 pptv dropping to 7 and 2 pptv for monthly and yearly averages, respectively. The ascending-descending systematic error biases were estimated to be less than ~3 pptv.

Zero order comparisons with the SCIAMACHY and OSIRIS datasets, as well as with the SLIMCAT and WACCM models were found to agree both in structure and in BrO magnitude. A more detailed validation is needed to properly asses the quality of these data. Nevertheless, we consider that this new dataset is usable for scientific studies. This dataset will be made publicly available for download in a daily based NetCDF format.

Using the WACCM and SLIMCAT Br_y/BrO modeled ratios we infer an estimate of stratospheric Br_y of 20.3 pptv with an error due to the MLS precision and systematics errors of 4.5 pptv. Assuming that the contribution of CH_3Br and halons to this Br_y budget was 15.6 pptv (Montzka et al., 2003) we derive a VSLS contribution to the total Br_y of $\sim 5 \pm 4.5$. This Br_y^{VSLS} estimate is well within the expected range found in WMO (2010, chaper 1).

Acknowledgements. The research described in this paper was carried out by the Jet Propulsion Laboratory, California Institute of Technology, under contract with the National Aeronautics and Space Administration. The SLIMCAT modelling work was supported by UK NERC NCAS and NCEO. The WACCM modelling work was sponsored by the National Science Foundation and by the NASA Atmospheric Composition: Modeling and Analysis, solicitation NNH10ZDA001N-ACMAP.

AMTD
5, 325–350, 2012

References

Bovensmann, H., Burrows, J. P., Buchwitz, M., Frerick, J., Noel, S., and Rozanov, V. V.: SCIAMACHY: mission objectives and measurement modes, J. Atmos. Sci., 56, 127–150, 1999.

Chipperfield, M. P.: Multiannual simulations with a three-dimensional chemical transport model, J. Geophys. Res., 104, 1781–1805, 1999. 332

Chipperfield, M. P.: New version of the TOMCAT/SLIMCAT off-line chemical transport model: intercomparison of stratospheric tracer experiments, Q. J. Roy. Meteor. Soc., 132, 1179–1203, 2006. 332

Engel, A., Strunck, M., Müller, M., Hasse, H.-P., Poss, C., Levin, I., and Schmidt, U.: Temporal development of total chlorine in the high-latitude stratosphere based on reference distributions of mean age derived from CO_2 and SF_6, J. Geophys. Res., 107, 4136, doi:10.1029/2001JD000584, 2002. 335

Farman, J. C., Gardiner B. G., and Shanklin, J. D.: Large losses of total ozone in Antartica reveal seasonal ClO_x/NO_x interaction, Nature, 315, 2007–2010, 1985. 326

Feng, W., Chipperfield, M. P., Dorf, M., Pfeilsticker, K., and Ricaud, P.: Mid-latitude ozone changes: studies with a 3-D CTM forced by ERA-40 analyses, Atmos. Chem. Phys., 7, 2357–2369, doi:10.5194/acp-7-2357-2007, 2007. 327

Garcia, R. R., Marsh, D., Kinninson, D. E., Boville, B., and Sassi, F.: Simulations of secular trends in the middle atmosphere, J. Geophys. Res., 112, D09301, doi:10.1029/2006JD007485, 2007. 332

Kinnison, D. E., Brasseur, G. P., Walters, S., Garcia, R. R., Marsh, D. R., Sassi, F., Harvey, V. L., Randall, C. E., Emmons, L., Lamarque, J. F., Hess, P., Orlando, J. J., Tie, X. X., Randel, W., Pan, L. L., Gettelman, A., Granier, C., Diehl, T., Niemeier, U., and Simmons, A. J.: Sensitivity of chemical tracers to meteorological parameters in the MOZART-3 chemical transport model, J. Geophys. Res., 112, D20302, doi:10.1029/2006JD007879, 2007. 333

Lamarque, J.-F., Emmons, L. K., Hess, P. G., Kinnison, D. E., Tilmes, S., Vitt, F., Heald, C. L., Holland, E. A., Lauritzen, P. H., Neu, J., Orlando, J. J., Rasch, P., and Tyndall, G.: CAM-chem: description and evaluation of interactive atmospheric chemistry in CESM, Geosci. Model Dev. Discuss., 4, 2199–2278, doi:10.5194/gmdd-4-2199-2011, 2011. 332

Kovalenko, L., Livesey, N., Salawitch, R., Camy-Peyret, C., Chipperfield, M., Cofield, R., Dorf, M., Drouin, B., Froidevaux, L., Fuller R., Goutail, F., Jarnot, R., Jucks, K., Knosp B., Lambert, A., MacKenzie, I., Pfeilsticker, K., Pommereau, J., Read, W., Santee, M.,

AMTD
5, 325–350, 2012

Schwartz, M., Snyder, W., Stachnik, R., Stek, P., Wagner, P., and Waters J.: Validation of Aura Microwave Limb Sounder BrO observations in the stratosphere, J. Geophys. Res., 112, D24S41, doi:10.1029/2007JD008817, 2007. 328, 329, 330, 335, 342

Llewellyn, E., Lloyd, N., Degenstein, D., Gattinger, R., Petelina, S., Bourassa, A., Wiensz, J., Ivanov, E., McDade, I., Solheim, B., McConnell, J., Haley, C., von Savigny, C., Sioris, C., McLinden, C., Grifoen, E., Kaminski, J., Evans, W., Puckrin, E., Strong, K., Wehrle, V., Hum, R., Kendall, D., Matsushita, J., Murtagh, D., Brohede, S., Stegman, J., Witt, G., Barnes, G., Payne, W., Pich, L., Smith, K., Warshaw, G., Deslauniers, D.-L., Marchand, P., Richardson, E., King, R., Wevers, I., McCreath, W., Kyrl, E., Oikarinen, L., Leppelmeier, G., Auvinen, H., Mgie, G., Hauchecorne, A., Lefvre, F., de La Ne, J., Ricaud, P., Frisk, U., Sjoberg, F., von Schele, F., and Nordh, L.: The OSIRIS instrument on the Odin spacecraft, Can. J. Phys., 82, 411–422, 2004. 334

Livesey, N., Kovalenko L., Salawitch, R., MacKenzie, I., Chipperfield, M., Read, W., Jarnot, R., and Waters, J.: EOS microwave limb sounder observations of upper stratospheric BrO: implications for total bromine, Geophys. Res. Lett., 33, L20817, doi:10.1029/2006GL026930, 2006a. 329, 335, 342

Livesey, N., Snyder, W. V., Read, W. G., and Wagner, P.: Retrieval Algorithms for the EOS Microwave Limb Sounder (MLS), IEEE T. Geosci. Remote, 44, 1144–1155, 2006b. 328

McLinden, C. A., Haley, C. S., Lloyd, N. D., Hendrick, F., Rozanov, A., Sinnhuber, B.-M., Goutail, F., Degenestein, D. A., Llewellyn, E. J., Sirios, C. E., Roozendael, M. V., Pommereau, J. P., Lotz, W., and Burrows, P.: Odin/OSIRIS observations of stratospheric BrO: retrieval methodology, climatology, and inferred Br_y, J. Geophys. Res., 115, D15308, doi:10.1029/2009JD012488, 2010. 334

Montzka, S. A., Butler, J. H., Hall, B. D., Mondeel, D. J., and Elkins, J. W.: A decline in tropospheric organic bromine, Geophys. Res. Lett., 30, 1826, doi:10.1029/2003GL017745, 2003. 326, 335, 336

Pundt, I., Pommereau, J.-P., Chipperfield, M. P., Van Roozendael M., and Goutail, F.: Climatology of the stratospheric BrO vertical distribution by balloon-borne UV-visible spectrometry, J. Geophys. Res., 107, 4806, doi:10.1029/2002JD002230, 2002. 327

Read, W., Lambert, A., Bacmeister, J., Cofield, R. E., Christensen, L. E. Cuddy, D. T., Daffer, W. H., Drouin, B. J., Fetzer, E., Froidevaux, L., Fuller, R., Herman, R., Jarnot, R. F., Jiang, J. H., Jiang, Y. B., Kelly, K., Knosp, B. W., Kovalenko, L. J. Livesey, N. J., Liu, H.-C., Manney, G. L., Pickett, H. M., Pumphrey, H. C., Rosenlof, K. H., Sabounchi, X.,

AMTD
5, 325–350, 2012

Santee, M. L., Schwartz, M. J., Snyder, W. V., Stek, P. C., Su, H. S., Takacs, L. L., Thurstans, R. P., Vömel, H., Wagner P. A., Waters, J. W., Webster, C. R., Weinstock, E. M., and Wu, D. L.: Aura microwave limb sounder upper tropospheric and lower stratospheric H_2O and relative humidity with respect to ice validation, J. Geophys. Res., 112, D24S35, doi:10.1029/2007JD008752, 2007. 331

Rodgers, C.: Inverse Methods for Atmospheric Sounding: Theory and Practice, Series on Atmospheric, Oceanic and Planetary Physics, vol. 2, World Scientific, Singapore, 2000. 328

Rozanov, A., Bovensmann, H., Bracher, A., Hrechanyy, S., Rozanov, V., Sinhuber, M., Stroh, F., and Burrows J. P.: NO_2 and BrO vertical profile retrieval from SCIAMACHY limb measurements: Sensitivity studies, Adv. Space Res., 36, 846–854, 2005. 333

Sander, S. P., Friedl, R. R., Ravishankara, A. R., Golden, D. M., Kolb, C. E., Kurylo, M. J., Huie, R. E., Orkin V. L., Molina, M. J., Moortgat, G. K., and Finlaysson-Pitts, B. J.: Chemical kinetics and photochemical data for use in atmospheric studies, Evaluation 14, JPL Publ., 02-25, Jet Propulsion Laboratory, Pasadena, California, 2003. 332

Sander, S. P., Friedl, R. R., Ravishankara, A. R., Golden, D. M., Kolb, C. E., Kurylo, M. J., Molina, M. J., Moortgat, G. K., Keller-Rudek H., Finlaysson-Pitts, B. J., Wine, P. H., Huie, R. H., and Orkin, V. L.: Chemical kinetics and photochemical data for use in atmospheric studies, Evaluation number 15, JPL Publ. 06-2, Jet Propulsion Laboratory, Pasadena, California, 2006. 333

Salawitch, R. J., Weisenstein, D. K., Kovalenko, L. J., Sioris, C. E., Wennberg, P. O., Chance, K., Ko, M. K. W., and McLinden, C. A.: Sensitivity of ozone to bromine in the lower stratosphere, Geophys. Res. Lett., 32, L05811, doi:10.1029/2004GL021504, 2005. 327

Sinnhuber, B.-M., Sheode, N., Sinnhuber, M., Chipperfield, M. P., and Feng, W.: The contribution of anthropogenic bromine emissions to past stratospheric ozone trends: a modelling study, Atmos. Chem. Phys., 9, 2863–2871, doi:10.5194/acp-9-2863-2009, 2009. 326

Soller, R., Nicovich, J. M., and Wine P. H.: Temperature-dependent rate coefficients for the reactions of Br($^2P_{3/2}$), Cl($^2P_{3/2}$), and O(^3P_J) with $BrONO_2$, J. Phys. Chem. A, 105, 1416–1422, 2001. 332

Wamsley, P. R., Elkins, J. W., Fahey, D. W., Dutton, G. S., Volk, C. M., Myers, R. C., Montzka, S. A., Butler, J. H., Clarke, A. D., Fraser, P. J., Steele, L. P., Lucarelli, M. P., Atlas, E. L., Schauffler, S. M., Blake, D. R., Rowland, F. S., Sturges, W W. T., Lee, J. M., Penkett, S. A., Engel, A., Stimpfle, R. M., Chan, K. R., Weisenstein D. K., Ko M. K. W., and Salawitch, R. J.: Distribution of halon-1211 in the upper troposphere and lower stratosphere

AMTD
5, 325–350, 2012

and the 1994 total bromine budget, J. Geophys. Res., 103, 1513–1526, 1998. 326
Waters, J., Read, W., Froidevaux, L., Jarnot, R., Cofield, R., Flower, D., Lau, G., Pickett, H., Santee, M., Wu, D., Boyles, M., Burke, J., Lay, R., Loo, M., Livesey, N., Lungu, T., Manney, G., Nakamura, L., Perun, V., Ridenoure, B., Shippony, Z., Siegel, P., Thurstans, R., Harwood, R., and Filipiak, M.: The UARS and EOS microwave limb sounder experiments, J. Atmos. Sci., 56, 194–218, 1999. 327
Waters, J., Froidevaux, L., Harwood, R., Jarnot, R., Pickett, H., Read, W., Siegel, P., Cofield, R., Filipiak, M., Flower, D., Holden, J., Lau, G., Livesey, N., Manney, G., Pumphrey, H., Santee, M., Wu, D., Cuddy, D., Lay, R., Loo, M., Perun, V., Schwartz, M., Stek, P., Thurstans, R., Boyles, M., Chandra, S., Chavez, M., Chen, G.-S., Chudasama, B., Dodge, R., Fuller, R., Girard, M., Jiang, J., Jiang, Y., Knosp, B., LaBelle, R., Lam, J., Lee, K., Miller, D., Oswald, J., Patel, N., Pukala, D., Quintero, O., Scaff, D., Snyder, W., Tope, M., Wagner, P., and Walch, M.: The Earth Observing System Microwave Limb Sounder (EOS MLS) on the aura satellite, IEEE T. Geosci. Remote, 44, 5, doi:10.1109/TGRS.2006.873771, 2006. 327
World Meteorological Organization: Scientific Assessment of Ozone Depletion: 2010, Global Ozone Research and Monitoring Project – Report No. 52, Geneva, Switzerland, 2010. 327, 335

AMTD
5, 325–350, 2012

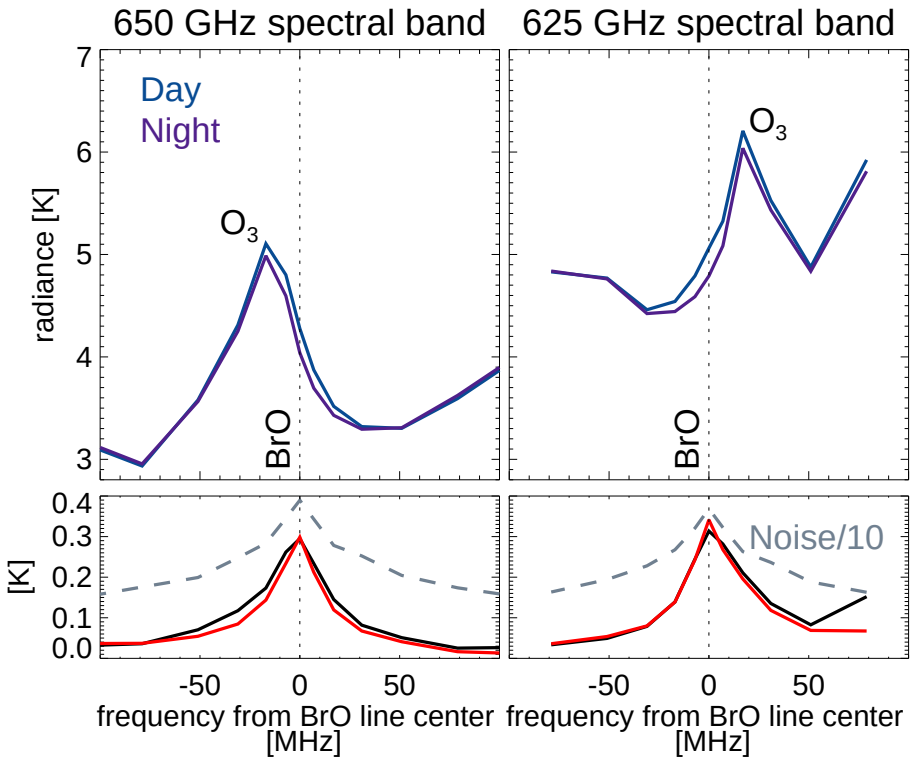

Fig. 1. (top) Average MLS radiance as detected in the 650 and 625 Ghz spectral bands sorted into day (blue) and night (purple) time measurements. Average is from 55° S and 55° N and for limb tangents from 10 to 4.6 hPa for 2005. (bottom) Differences between the ascending and descending (mainly day and mainly night) measurements (black) reveals the BrO spectral signature. The red lines represent the spectrum simulated by using the new averaged BrO retrieved value introduced here. The dashed gray line is 1/10 of the expected single scan noise, which is still greater than the BrO signal.

AMTD
5, 325–350, 2012

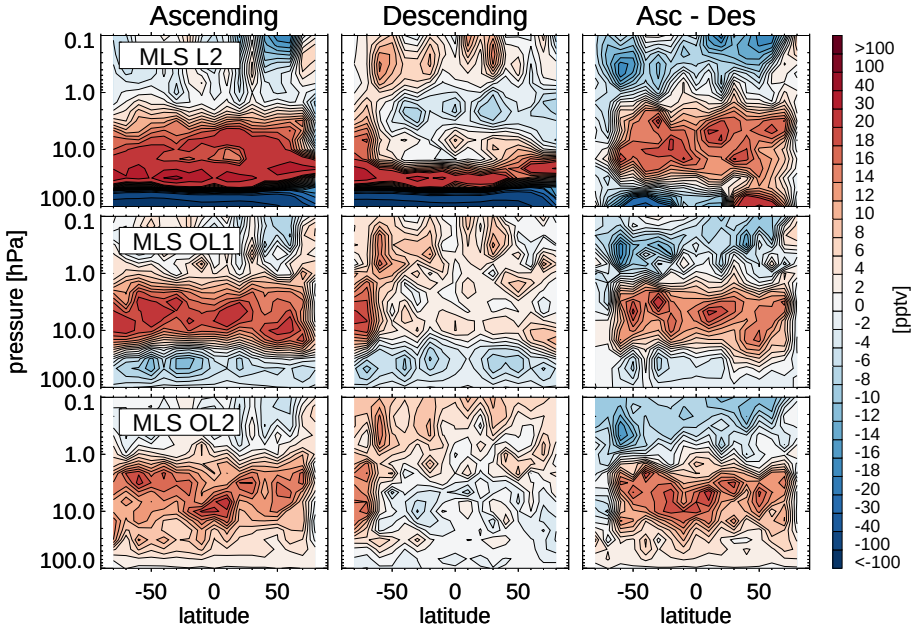

Fig. 2. Monthly zonal mean for January 2005 of MLS BrO observations for the three versions discussed in the text for ascending (mainly daytime) and descending (mainly nighttime) phases of the orbit. The dataset MLS L2 is the standard production algorithm described by Kovalenko et al. (2007), MLS OL1 is the "off-line" algorithm described by Livesey et al. (2006a) and MLS OL2 is the dataset introduced here.

AMTD
5, 325–350, 2012

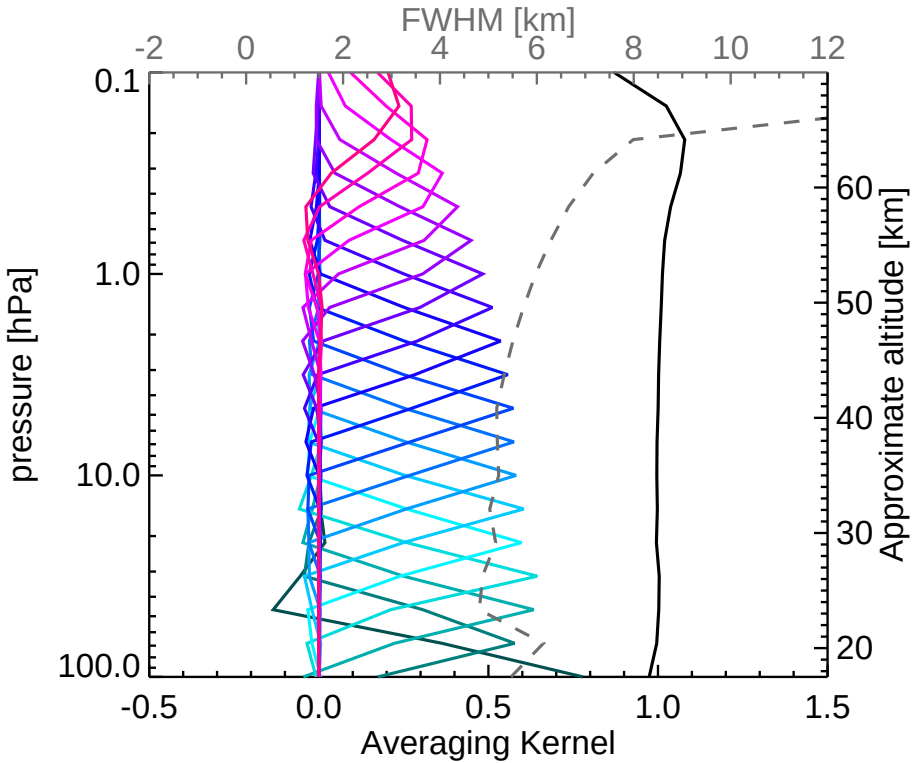

Fig. 3. Averaging kernels for the retrieval of BrO mixing ratio at the Equator (those at other latitudes are very similar). The black line is the integrated area under each kernel: values near unity indicate that most information was provided by the measurements while lower values indicate that the retrieval was influenced by the a priori. The dashed gray line is a measure of the vertical resolution of the retrieved profile (derived from the full width at half maximum (FWHM) of the averaging kernels approximately scaled into kilometers).

AMTD
5, 325–350, 2012

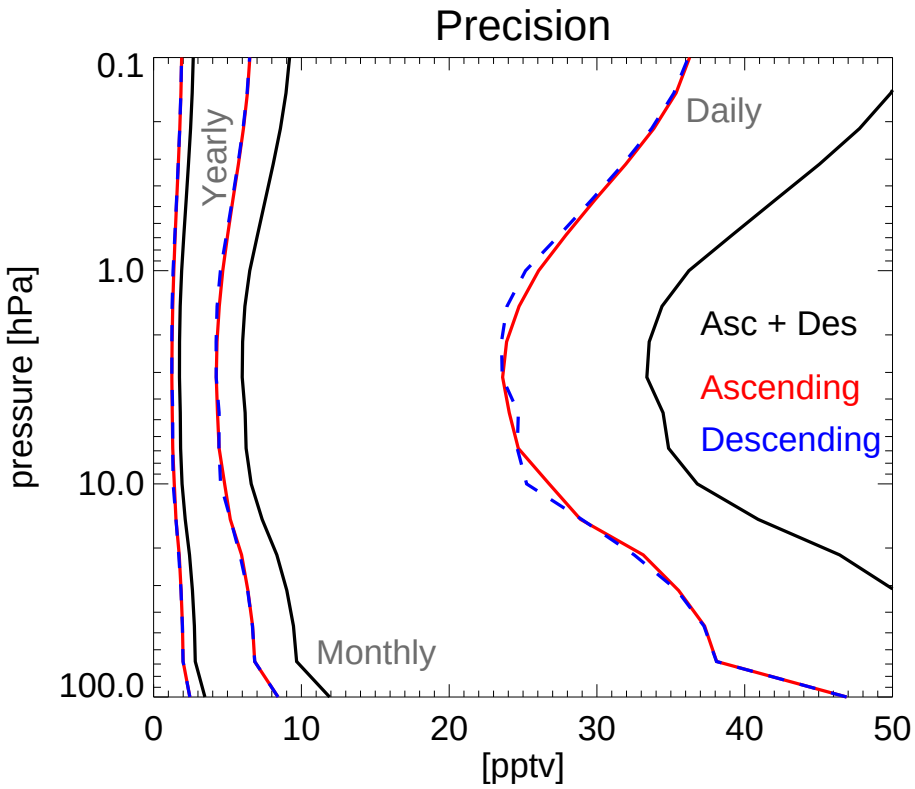

Fig. 4. Expected precision for a daily, monthly and yearly 10° latitude bin. The "Asc + Des" precision is the root sum square of the ascending and descending values.

AMTD
5, 325–350, 2012

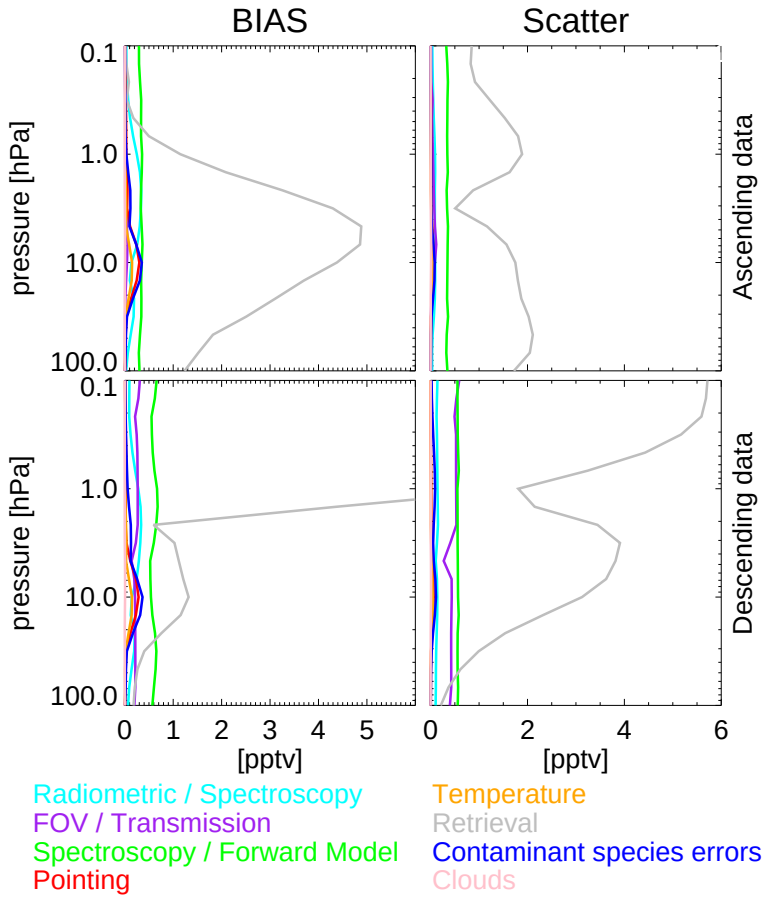

Fig. 5. Estimated impact of various families of systematic errors on the MLS OL2 BrO "off-line" observations. The top panel corresponds to the ascending part of the orbit while the lower panel corresponds to the descending part. The left panel shows the possible biases and the right panel shows the additional scatter introduced by each family of systematic errors.

AMTD
5, 325–350, 2012

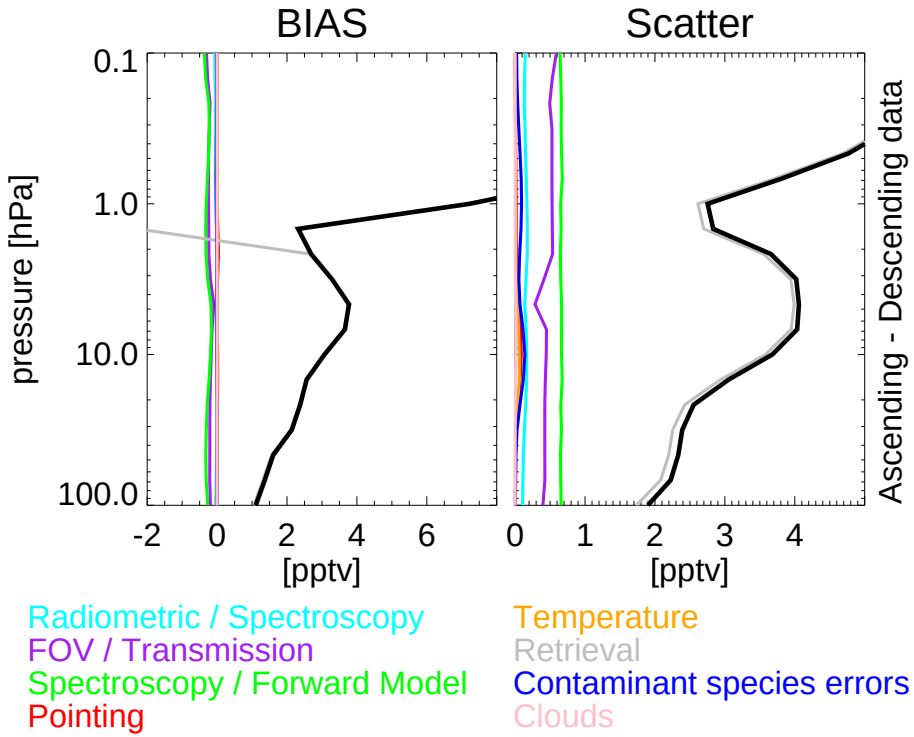

Fig. 6. Estimated impact of various families of systematic errors for ascending–descending MLS OL2 BrO observations. The left panel shows the possible biases (the difference of the ascending-descending biases in Fig. 5) and the right panel shows the additional scatter introduced by each family of systematic errors (the root sum squares of the scatter in Fig. 5). The black lines are the root sum squares of all the biases or the scatters shown.

AMTD
5, 325–350, 2012

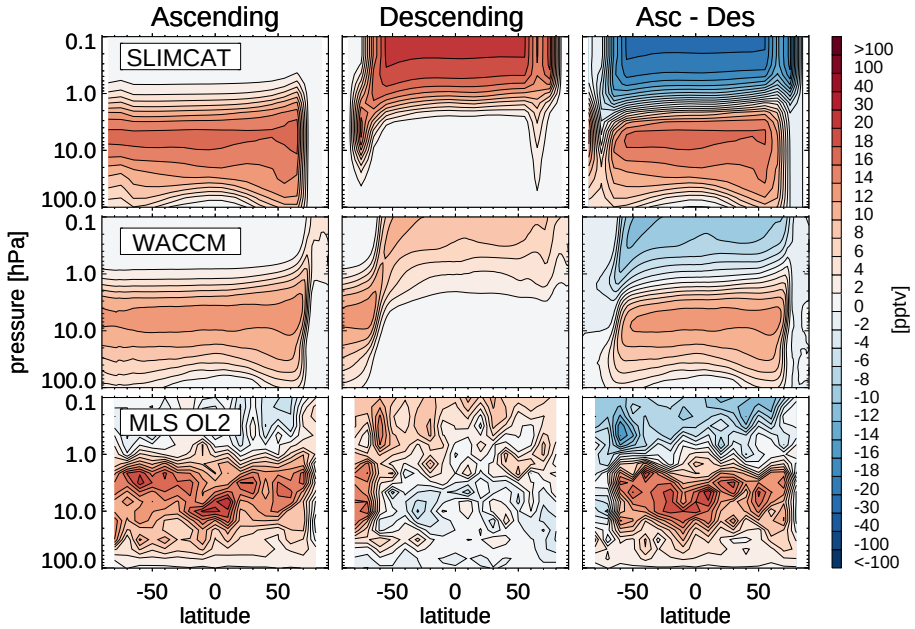

Fig. 7. Monthly zonal mean of MLS BrO observations for ascending and descending phases of the orbits as well as the SLIMCAT and WACCM models for January 2005. To alleviate biases in the MLS BrO data, the ascending/descending differences are used as a measure of daytime BrO for pressure greater than ~4 hPa where the nightime BrO is expected to be zero.

AMTD
5, 325–350, 2012

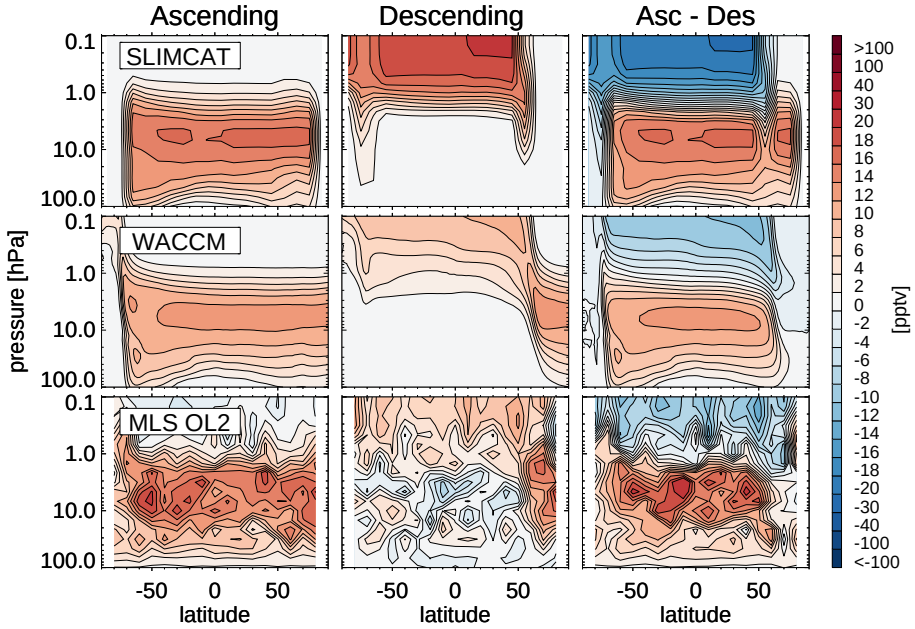

Fig. 8. Same as Fig. 7, except that the data correspond to July instead of January 2005.

AMTD
5, 325–350, 2012

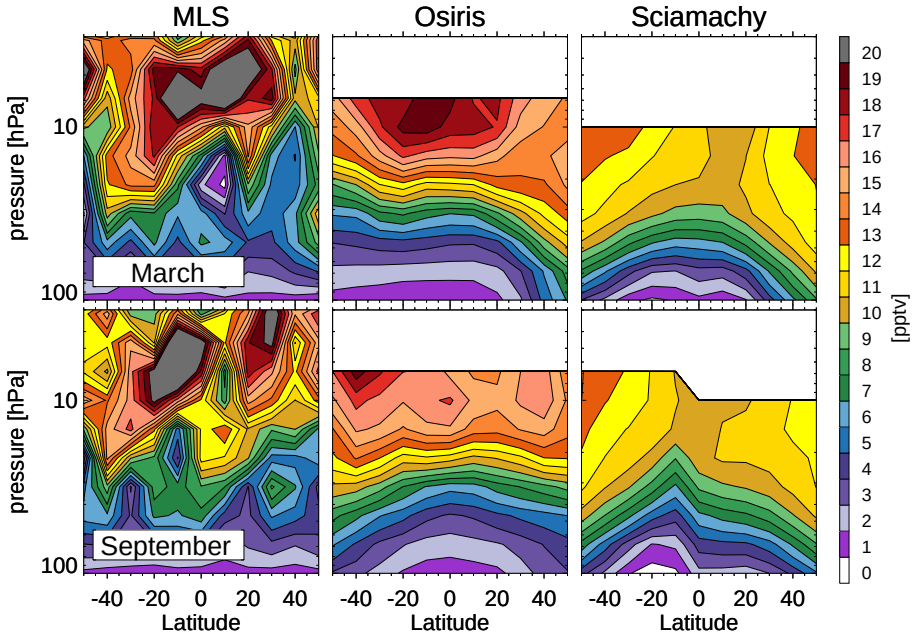

Fig. 9. Monthly zonal mean of MLS (Asc–Des), OSIRIS and SCIAMACHY BrO observations for March and September 2005. These datasets are in different local times (1:45 p.m., 6 a.m. and 10 a.m., respectively) so exact agreement is not expected.

AMTD
5, 325–350, 2012

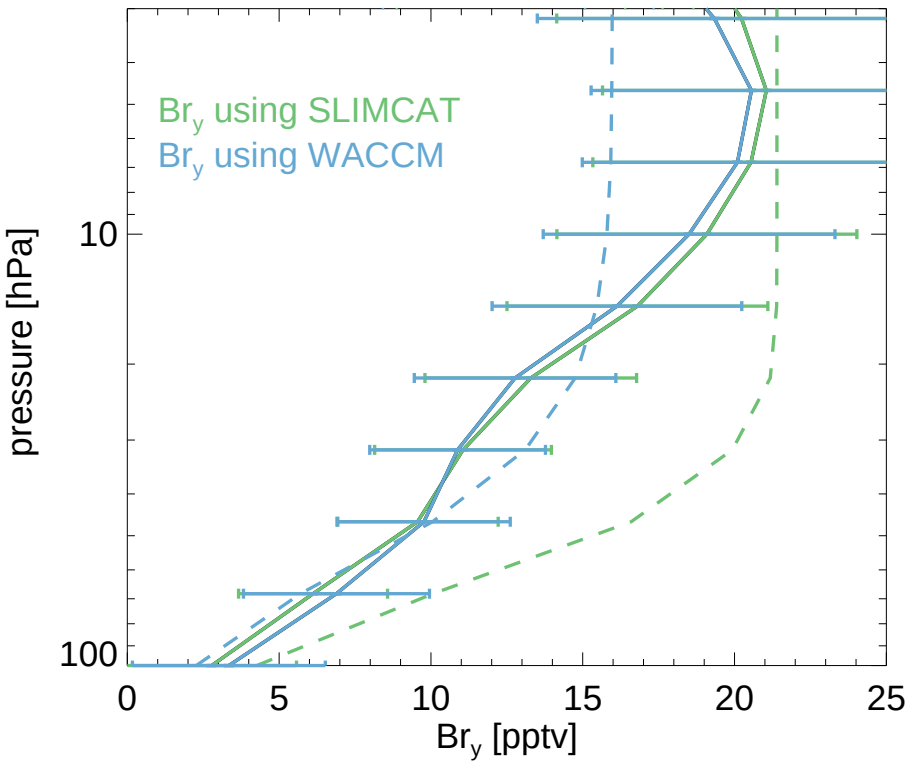

Fig. 10. Average Br$_y$ inferred from MLS data using the SLIMCAT (green) and the WACCM (blue) models as described by Eq. (2). Average is for the year 2005. The error bars reflect the total errors (a combination of the measurement errors and the systematic errors). For comparison, the dashed lines show the SLIMCAT (green) and WACCM (blue) modeled values.

AMTD
5, 325–350, 2012